Fast deformation of shocked quartz and implications for planar deformation features observed in shocked quartz

HPSTAR 1055-2020

Cite as: AIP Conference Proceedings **2272**, 080002 (2020); https://doi.org/10.1063/12.0000930
Published Online: 04 November 2020

Toshimori Sekine, Tomoko Sato, Norimasa Ozaki, Kohei Miyanishi, Ryosuke Kodama, Yusuke Seto, Yoshinori Tange, Subodh C. Tiwari, Aiichiro Nakano, and Priya Vashishta

Fast Deformation of Shocked Quartz and Implications for Planar Deformation Features Observed in Shocked Quartz

Toshimori Sekine[1, 2, a)], Tomoko Sato[3], Norimasa Ozaki[2], Kohei Miyanishi[2], Ryosuke Kodama[2], Yusuke Seto[4], Yoshinori Tange[5], Subodh C. Tiwari[6], Aiichiro Nakano[6], and Priya Vashishta[6]

[1]*Center for High Pressure Science & Technology Advanced Research, Shanghai 201203, China,*
[2]*Graduate School of Engineering, Osaka University, Suita 565-0871, Japan,*
[3]*Department of Earth & Planetary Systems Science, Hiroshima University, Higashi-Hiroshima 739-8526, Japan,*
[4]*Graduate School of Science, Kobe University, Kobe 657-8501, Japan,*
[5]*Japan Synchrotron Radiation Research Institute (JASRI), Sayo-cho, Hyogo 679-5198, Japan,*
[6]*Collaboratory for Advanced Computing & Simulations, Department of Physics & Astronomy, Department of Computer Science, Department of Chemical Engineering and Materials Science, and Department of Biological Science, University of Southern California, Los Angeles, CA 90089–0242, USA*

[a)]*Corresponding author: toshimori.sekine@hpstar.ac.cn*

Abstract. Fast deformations in the quartz crystals during shock compression process have been investigated with two time-resolved methods of *in-situ* diffractions by x-ray free electron laser (XFEL) and large-scale molecular dynamic (MD) simulations in order to get insights in planar deformation feature (PDF) mechanism. PDFs in quartz provide strong evidence for impact and are used to estimate the impact conditions. The present experimental results on X-cut and Y-cut quartz single crystals at pressures below phase transition indicate ideal uniaxial compression and rotation of fractured grains to a direction to heat up locally due to dispersed particle velocity distribution in the dynamic movement. This could explain the observed disordering at given planes, as supported by the MD simulations.

INTRODUCTION

According to many intensive studies on meteorites and impactites that experienced impacts, quartz (Qz) crystal exhibits a series of residual shock effects, including fractures, planar microstructures, mosaicism, amorphization, high-pressure phases (coesite, stishovite and seifertite) and melting, as a function of the peak shock pressure. The residual effects are used to estimate the shock intensity they experienced. According to the results on Hugoniot measurements [1, 2] and shock recovery experiments [3, 4, 5] of quartz, the shock response of quartz can be modeled as the low pressure (LP) and mixed phase (MP) regions below ~40 GPa, dependent on the crystal orientation, and the high pressure form (HP) is realized above a pressure of ~15 GPa [6, 7]. The shock effects observed in Qz at the LP are produced irregular, non-planar fractures, planar fractures (PF) parallel to the crystallographic planes with low Miller indices, and planar deformation features (PDF) as multiple sets of parallel, planar optical discontinuities. From comparisons of PDFs in Qz between natural and shock recovered samples, some of PDFs may be produced by thermal annealing of primary PDFs. Langenhorst (1994) [8] described amorphous lamellae of thin (~30 nm) straight, planar one at < 25 GPa and thick (~200 nm) one with wavy boundaries at >25 GPa, based on the observations of experimentally-shocked Qz by transmission electron microscopy (TEM). There are many x-ray diffraction characterizations on shocked Qz for 50 years (e.g. refs. 9; 10). These studies have tried to estimate the average shock pressures from the shocked Qz [11]. However, there is no in-situ experimental trial how the deformation and PDF form to evolve during shock compression process. We need to know the formation

Shock Compression of Condensed Matter - 2019
AIP Conf. Proc. 2272, 080002-1–080002-5; https://doi.org/10.1063/12.0000930
Published by AIP Publishing. 978-0-7354-4000-5/$30.00

mechanism and the quenching process during pressure release using *in-situ* time-resolved techniques. Here we adopt two *in-situ* techniques of a direct x-ray diffraction method during shock compression of single crystal Qz and a large-scale molecular dynamics simulation.

Quartz is an important geological material that has been subjected to extensive investigations both experimentally and theroretically. However only a few studies on the phase transition under shock compressions are available using intensive bright x-ray and most of the previous studies focused on polycrystalline quartz [12]. There is no in-situ, lattice-level observation for the deformation under shock loadings that can be visualized by femtosecond bright x-ray free electron laser (XFEL) using a single crystal quartz and a large-scale molecular dynamic (MD) simulation. It is challenging to study single crystal quartz by XFEL. We try to understand the formation mechanism based on the time-resolved x-ray diffraction and simulation methods recently available.

EXPERIMENTAL

We used two types of X-cut and Y-cut single crystal Qz (50 μm thick). They are shocked normal and perpendicular to the (200) plane by an optical laser and measured by diffractions using the XFEL at Spring-8 Angstrom Compact Free-electron Laser (SACLA) [13]. The optical laser is a chirped Ti: sapphire laser (~600 ps pulse, wavelength 800 nm, ~1 J/pulse, focused ~0.4 μm in diameter on target under vacuum chamber at an average intensity of ~2 x 10^{12} W/cm^2). SACLA XFEL is 8 fs pulse, 0.9 mJ/pulse, 10 keV photon energy with ~10^{11} photons per pulse, focused in one direction down to ~17 μm using a Kirkpatrick-Baez (KB) mirror, whereas the other axis was adjusted to ~200 μm by a two-quadrant slit. The target was placed at a 20° incident angle compared to the XFEL beam axis (Fig. 1). The diffraction data was observed on a one-megapixel array detector [14] to measure the lattice spacing (200) of single crystal Qz by changing the angle between x-ray beam and sample gradually at a time day, thus obtaining variations of the diffraction images give us detailed shifts of the diffraction peak including grain rotation around the x-ray beam. The timing jitter was within 100 ps. We calculated the shock state using MULTI code [15] to guide experimental setup.

In the present study, the simulated systems are Qz single crystal slabs of about 29 x 29 x 185 nm^3 containing ~11 million atoms. The long system dimension, along the [210] direction of Qz, is aligned with the impact direction to allow the shock waves to develop for at least 24.5 ps. After that the system is subject to rarefaction. The Si-O bond is characterized by the number of oxygen atoms around Si atom (coordination number=CN) and by the shearing conditions of corner and edge among the tetrahedron (CN=4), pyramid (CN=5), and octahedron (CN=6) [16]. Before impact, the crystalline structure of the target material is a defect-free Qz. The planar impact simulations are performed in the reversed geometry with the system target hitting the piston at a fixed position with a chosen impact velocity. The piston is modeled as a hard wall, which instantly bounces any particle hitting its surface by inverting the component of the momentum perpendicular to the hard wall. Shock profile of properties is calculated along the system in the impact z direction. The equations of motion are numerically integrated using the velocity-Verlet algorithm with a time step of 1 fs. For the range of impact velocities investigated this time step is small enough to allow stable integration of the equations of motion for all atoms and the conservation of the energy during all simulations. The pressures are 13-25 GPa. The purpose was to quantify the *in-situ* bonding dynamics in shocked Qz and non equilibrium molecular dynamics refined with QMD method is most suitable [16].

RESULTS AND DISCUSSION

Figure 1 illustrates Bragg and Laue geometries to measure the diffraction from the plane (200) of the whole 50 μm thickness used in the present study. The plane with d_o=2.129 Å is compressed normally in the Bragg geometry and parallel in the Laue one, respectively. The diffraction patterns for the Bragg geometry at 1 ns showed a simple compression movement of diffraction image and the observed maximum values of d_0/d was 0.83. The observed values of d_0/d were 0.89 and 0.98 at 7.2 ns for the two geometries respectively because the partially released state started at 7.2 ns. According to the quartz Hugoniot, the peak stress is ~18 GPa at 1 ns and ~10 GPa at 7.2 ns, although the Hugoniot compression curve [1] indicates little change between X-cut and Y-cut quartz crystals. The present results indicate a large difference between the two orientations. This may suggest that Hugoniot depends upon strain rate because the deformation and phase transition depend on the strain rate.

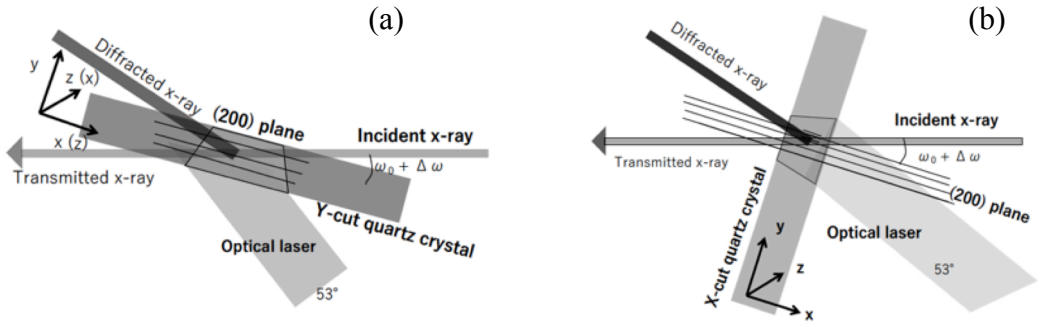

FIGURE 1. Two target geometries of (a) Bragg and (b) Laue used in the present study. By changing Δω around 17 degree against the incident x-ray beam, the slight mismatching diffraction image can be visualized. The interspacing (200) was measured at various delay times during laser-shock of the quartz crystal. Target crystal was replaced after each shot.

As illustrated in Fig. 2, the Bragg geometry patterns at a delay time (7.2 ns) showed very unique variation with Δω that gives us the detailed diffraction image for the fixed diffraction peak (200). At relatively low Δω (0.5–1.4 degree), the images contain the parts at ambient and relatively weak compressed components, and the most compressed position is isolated from the ambient position. At 0.8 degree Δω, the side image shows fine structures with intermediately compressed area located at the right hand side. This may indicate mosaic spread and rotation near ambient state. At high Δω (1.7 and 2.0), the compressed diffraction extended to the right hand side is seen without ambient diffraction. Such diffraction images using synchrotron beams have been known as grain rotation around the x-ray beam [17]. Taking into account that Laue geometry showed large spotty images only and did not show significantly grain rotation, the rotation may occur only in the plane and mainly at a direction based on the observed image that indicates stronger diffraction at the right side than the left side. Energetically it seems to be balanced in the rotations between near ambient and on release. Further these movements were observed during the release state and not at the compression processes. These results do not indicate any amorphization in shocked quartz clearly due to too small amount, but rapid rotations in planes may initiate locally frictional heating between planes. These can be explained by local variations of particle velocity in Qz. Fracturing during shock compression makes grain contacts like polycrystals. It has been known that dispersed particle velocity in polycrystalline metals brings local turbulence in motion [18]. Further studies require to understand the PDF formation mechanism in detail. Next we tried to simulate with a large-scale molecular dynamic method.

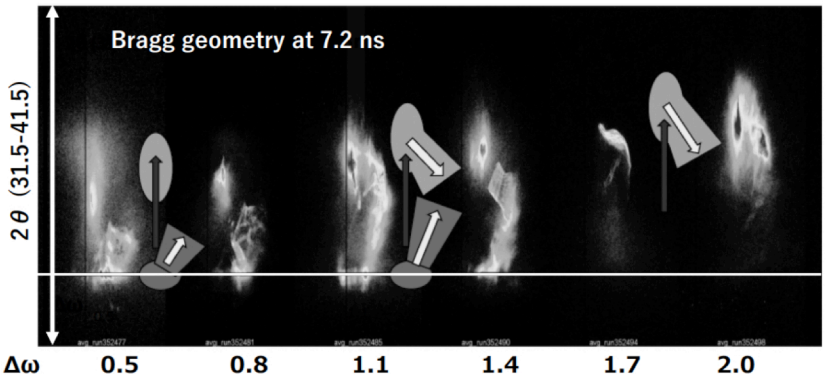

FIGURE 2. A series of quartz (200) diffraction images at various Δw values for Bragg geometry when the quartz is subjected to partial release at a delay time of 7.2 ns. The vertical axis is 2θ of 31.5 to 41.4 degree, and the horizontal line is the position at the ambient pressure. Note that there are two evolutional trends of a vertical extension (compression) and an enlargement to the right hand (rotation and mosaic spread) during compression and release, marked by arrows .

Figure 3 shows the pressure profiles for given particle velocity (Up) of 1.2 km/s-1/8 km/s at 24.5 ps. At Up =1.2 km/s, the initially generated pressure drops gradually and increases. The profiles at Up > 1.3 km/s indicate two waves clearly. The shock velocity for the first wave is reduced slightly with increasing Up in the present range of Up. At 1.2 km/s Up, it appears to take long time for new bond of Si-O to be created and the equilibrium does not reach.

Although the nucleation and growth rate increase with increasing the given Up as illustrated in Fig. 4, the actual process may be more complicated than what the available Hugoniot data indicate. The transformation to the pyramidal (and very locally octahedral) units is seen at the second compression state and it reverts to the tetrahedral units during release. It is noteworthy that multiple grains grow along the [100] direction and they make amorphous grain boundaries with specific angles. The average calculated temperature indicates that systems are significantly below the melting curve, and amorphization occur as solid-solid reaction. Grain rotation in a plane during shock compression can make locally frictional heating at the plane as well [18] even in a single crystal that displays subsequent mosaic spread at the late stage.

These conditions and *in-situ* structural changes at the atomic level in shocked Qz can be directly compared with the PDFs observed in natural Qz that experienced impact. Taking into account that the presence of PDFs in Qz is an evidence for strong impact, we need further study to unravel the detailed relation between the multiple PDF distributions and peak shock pressure as well as pressure duration.

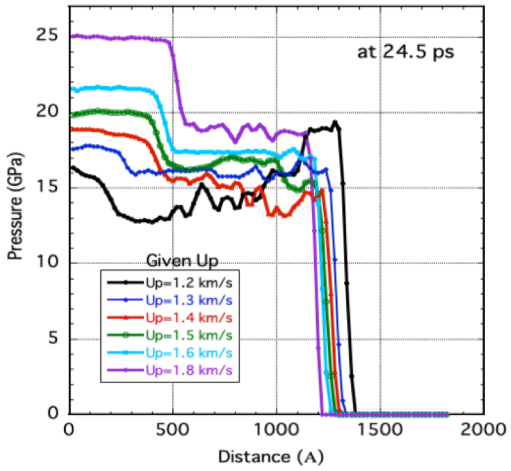

FIGURE 3. Simulated profiles of pressure-distance in single crystal quartz (29 nm x 29 nm x 185 nm) compressed along [210] at given particle velocities of 1.2-1.8 km/s at a delay time of 24.5 ps. Note two-shockwave structure. After plastic compression, the coordination number (CN) around Si atom increases 5 in the [100] plane as multiple grains. Each grain with CN=5 is released as amorphous [19].

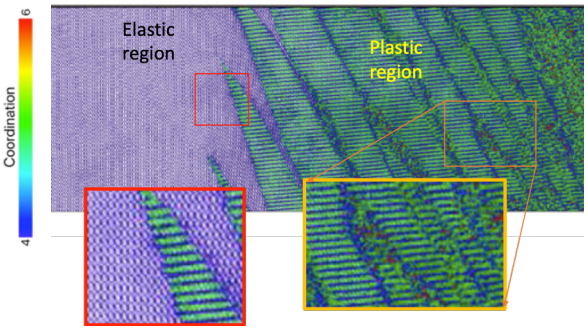

FIGURE 4. Snapshot of MD simulations showing the transformation of tetrahedral Si to pyramidal Si (and octahedral Si) by plastic wave around 20 GPa, when a single crystal quartz is compressed along [210]. After release it retrieves as the tetrahedral Si. The bottom inserts illustrate areas at the front of the elastic wave and within a typical interior.

ACKNOWLEDGMENTS

We are thankful for the SACLA operation team and participant students from Osaka University and Hiroshima University. The SACLA proposal number is 2015A8065. We thank Paulo Branicio at USC for his contributions in the simulation. This research supported by JSPS Core-to Core Program on International Alliance for Material Science in Extreme State with High Power Laser and FEEL and a MEXT project.

REFERENCES

1. J. Wackerle, J. Appl. Phys. **33**, 922-937 (1962).
2. R. Fowler, J. Appl. Phys. **72**, 5729-5742 (1967).
3. P.S. DeCarli and J.C. Jamieson, J. Chem. Phys. **31**, 1675-1676 (1959).
4. P.S. DeCarli and D.J. Millton, Science **147**, 144-145 (1965).
5. T. Sekine, M. Akaishi and N. Sedaka, Geochim. Cosmochim. Acta **51**, 379-381 (1987).
6. J. W. Swegle, J. Appl. Phys. **68**, 1563-1579 (1990).
7. J.C. Boettger, J. Appl. Phys. **72**, 5500-5508 (1992).
8. F. Langenhorst, Earth Planet. Sci. Lett. **128**, 683-698 (1994).
9. L. Ferrière, J.R. Morrow, T. Amgaa, and C. Koberl, Met. Planet. Sci. **44**, 925-940 (2009).
10. R.E. Hanss, B.R. Montague, M.K. Davis, and C. Galindo, Proc. Lunar Planet Sci. Conf. 9th, 2773-2787 (1978).
11. D. Stöffler and F. Langenhorst, Met. Planet. Sci. **29**, 155-181 (1994).
12. A.E. Gleason, C.A. Bolme, H.J. Lee, B. Nagler, E. Galtier, D. Milathianaki, J. Hawreliak, R.G. Kraus, J.H. Eggert, D.E. Fratanduono, G.W. Collins, R. Sandberg, W. Yang, and W.L. Mao, Nature Commun. **6**, 8191 (2015)
13. K. Tono, T. Togashi, Y. Inubushi, T. Sato, T. Katayama, K. Ogawa, H. Ohashi, H. Kimura, S. Takahashi, K. Takeshita, H. Tomizawa, S. Goto, T. Ishikawa, and M. Yabashi, New J. Phys. **15**, 083035 (2013).
14. T. Kameshima, S. Ono, T. Kudo, K. Ozaki, Y. Kirihara, K. Kobayashi, Y. Inubushi, M. Yabashi, T. Horigome, A. Holland, K. Holland, D. Burt, H. Murao, and T. Hatsui, Rev. Sci. Instrum. **85**, 033110 (2014).
15. R. Ramis, R. Schmalz and J. Meyer-Ter-Vehn, Comp. Phys. Commun. **49**, 475 (1988).
16. M. Misawa, E. Ryuo, K. Yoshida, R.K. Kalia, A, Nakano, N. Nishiyama, F. Shimojo, P. Vashishta, and F. Wakai, Sci. Adv. **3**, e1602339.
17. K-D Liss and K. Yan, Mat. Sci. Eng. A**528**, 11-27 (2010).
18. Y. Yano and Y. Horie, Phys. Rev. B59, 13672-13680 (1999).
19. S.T. Tiwari, M. Misawa, T. Sato, F. Shimojo, A. Nakano, T. Sekine, P. Branicio, and P. Vashishta, Poster presentation at APS Spring meeting 2019.